Published online 12 December 2017 *Nucleic Acids Research, 2018, Vol. 46, No. 3* ***1501–1512***
doi: 10.1093/nar/gkx1234

A peculiar IclR family transcription factor regulates *para*-hydroxybenzoate catabolism in *Streptomyces coelicolor*

Rui Zhang[1], Dana M. Lord[2], Rakhi Bajaj[3,4], Wolfgang Peti[2,4], Rebecca Page[3,4,*] and Jason K. Sello[1,*]

[1]Department of Chemistry, Brown University, Providence, RI 02912, USA, [2]Department of Molecular Pharmacology, Physiology, and Biotechnology, Brown University, Providence, RI 02912, USA, [3]Department of Molecular Biology, Cell Biology, and Biochemistry, Brown University, Providence, RI 02912, USA and [4]Department of Chemistry and Biochemistry, University of Arizona, 1041 E. Lowell St., Tucson, AZ 85721, USA

Received August 31, 2017; Revised November 20, 2017; Editorial Decision November 24, 2017; Accepted December 08, 2017

ABSTRACT

In *Streptomyces coelicolor,* we identified a *para*-hydroxybenzoate (PHB) hydroxylase, encoded by gene *pobA* (SCO3084), which is responsible for conversion of PHB into PCA (protocatechuic acid), a substrate of the *β*-ketoadipate pathway which yields intermediates of the Krebs cycle. We also found that the transcription of *pobA* is induced by PHB and is negatively regulated by the product of SCO3209, which we named PobR. The product of this gene is highly unusual in that it is the apparent fusion of two IclR family transcription factors. Bioinformatic analyses, *in vivo* transcriptional assays, electrophoretic mobility shift assays (EMSAs), DNase I footprinting, and isothermal calorimetry (ITC) were used to elucidate the regulatory mechanism of PobR. We found that PobR loses its high affinity for DNA (*i.e.,* the *pobA* operator) in the presence of PHB, the inducer of *pobA* transcription. PHB binds to PobR with a K_D of 5.8 μM. Size-exclusion chromatography revealed that PobR is a dimer in the absence of PHB and a monomer in the presence of PHB. The crystal structure of PobR in complex with PHB showed that only one of the two IclR ligand binding domains was occupied, and defined how the N-terminal ligand binding domain engages the effector ligand.

INTRODUCTION

Aromatic compounds are among the most abundant forms of carbon on the planet. They have a wide range of structures and origins (1–3). For example, lignin is a polyoxygenated, aromatic polymer produced by plants that makes up 25% of the biomass on land (4). The environment is also replete with anthropogenic aromatic compounds, like polyaromatic hydrocarbons derived from fossil fuel utilization and pesticides (5–7). Aromatic compounds are notoriously stable, yet they do not persist in the environment due to the capacities of microorganisms to catabolize them. Studies of terrestrial bacteria and fungi have revealed sophisticated and varied catabolic pathways through which they consume aromatic compounds of both natural and human origins (8,9). Catabolism of structurally diverse aromatics in bacteria often yields catechol and protocatechuic acid (PCA) (9,10). Interestingly, these aromatic compounds are enzymatically converted to intermediates of the Krebs cycle via three distinct catabolic pathways (10). The most predominant involves the 3,4-cleavage of the diol and the subsequent conversion to β-ketoadipate. The eponymous β-ketoadipate pathway ultimately yields succinate and acetyl coenzyme A. The other commonly observed catabolic pathways are defined by 2,3-cleavage (11–13) or 4,5-cleavage of PCA (14). The former converts PCA to pyruvate and acetyl coenzyme A, while the latter yields pyruvate and oxaloacetate (10). These pathways endow microorganisms with the capacity to flux the carbon of aromatic compounds into intermediary metabolism underlying growth and reproduction (8).

Because aromatic compound catabolism requires many highly reactive enzymes and is secondary to carbohydrate consumption, microorganisms tend to exert tight regulatory control over it (15,16). Indeed, regulation of aromatic catabolism is typically mediated at the level of gene transcription (15–18). As shown in Supplementary Table S1, transcription factors regulating this phenomenon in bacteria act either positively or negatively and can be assigned to one of the well-known families (15,17,18). In bacteria, the widely distributed *β*-ketoadipate pathway for aromatic

*To whom correspondence should be addressed. Tel: +1 401 863 1194; Fax: +1 401 863 9046; Email: jason_sello@brown.edu
Correspondence may also be addressed to Rebecca Page. Tel: +1 520 626 0389; Fax: +1 520 626 0389; Email: rebeccapage@email.arizona.edu

catabolism is regulated by members of multiple families of transcription factors (*i.e.*, LysR, IclR and MarR) (17,18). Interestingly, members of the LysR and IclR families are all transcriptional activators, whereas the MarR family contains both transcriptional activators and repressors. Mechanistic studies of these proteins have provided important insights into the regulation of gene expression in bacteria (15).

A molecular understanding of aromatic catabolism and its regulation could be exploited in the engineering of microorganisms to convert the cheap and readily abundant aromatic compounds into commodity chemicals and biofuels. In this context, we have been interested in the catabolism of *para*-hydroxybenzoate (PHB) by *Streptomyces* bacteria. PHB, a well-known product of the microbial degradation of lignin, is highly abundant and cheap (19). It is converted by *para*-hydroxybenzoate hydroxylase to PCA, an expensive and key intermediate in aromatic catabolism (19–24). We studied PHB catabolism in streptomycetes because these bacteria are known to produce commodity chemicals (*e.g.*, antibiotics) and are amenable to genetic manipulation. Importantly, there is a wealth of information about aromatic catabolism and its regulation in these organisms.

Our studies of PHB catabolism were carried out in *Streptomyces coelicolor*, the model organism of the genus. A bioinformatic analysis of its genome revealed the presence of two paralogous genes (SCO1308 and SCO3084) encoding putative *p*-hydroxybenzoate hydroxylases, the products of which are homologous to the flavin-dependent monooxygenases known as PobA in *Pseudomonas fluorescens* and *Pseudomonas aeruginosa*. A second bioinformatic analysis focused on the identification of transcription factors reminiscent of those known to regulate *pobA* orthologs revealed two genes, SCO0266, which encodes a putative transcriptional regulator that is homologous to PobR from *Pseudomonas sp.* Strain HR199, and SCO3209, which appeared to be a head-to-tail translational fusion of two transcription factors that are homologous to the regulator of *pobA* expression known as PobR in *Acinetobacter calcoaceticus*. The homologies and redundancies of the *pobA* and *pobR* orthologs in *S. coelicolor* motivated us to use genetic, biochemical, and biophysical experiments to define the hypothetical roles of their products in PHB catabolism and its regulation. Thus, we determined the genetic basis of *p*-hydroxybenzoic acid catabolism in *S. coelicolor* and how it is regulated by a novel transcription factor that is unique among IclR family members. These findings set the stage for the genetic engineering of bacteria to convert aromatic compounds to commodity chemicals.

MATERIALS AND METHODS

Bacterial strains and culture conditions

A complete list of bacterial strains employed in this study is provided in Supplementary Table S2. *Escherichia coli* strains DH5α, ET12567/pUZ8002 and BL21-Gold (DE3) were grown on Luria-Bertani medium at 37°C for routine sub-cloning (25), while *E. coli* strain BW25113/pIJ790 was grown at 30°C to maintain selection of pIJ790. *S. coelicolor* strains were grown at 30°C on solid mannitol soya flour medium (SFM), liquid yeast extract-malt extract medium (YEME), liquid minimal liquid medium (NMMP) (26) or solid minimal medium (MM) [3 g Gelzan (a poorly catabolized alternative to agar), 1 g $(NH_4)_2SO_4$, 5 g K_2HPO_4, 2 g $MgSO_4{\cdot}7H_2O$, 0.1 g $FeSO_4{\cdot}7H_2O$ per liter]. For minimal medium, carbon sources were sterilized separately and added to media at the following final concentrations: glucose, 5 g per liter; *para*-hydroxybenzoate (PHB), 20 mM; protocatechuic acid (PCA), 20 mM; and 1% (vol/vol) EtOH as negative control. Genomic DNA was isolated from *S. coelicolor* grown in YEME and total mRNA was isolated from *S. coelicolor* grown in NMMP. MM was used in experiments for definition of aromatic compounds that support growth of *S. coelicolor*. For selection of *E. coli*, antibiotics were used at the following concentrations: ampicillin (100 μg/mL), apramycin (50 μg/mL), chloramphenicol (25 μg/mL), hygromycin (75 μg/mL), kanamycin (50 μg/mL), spectinomycin (50 μg/mL) and streptomycin (50 μg/mL). For selection of *S. coelicolor*, apramycin (50 μg/mL), hygromycin (75 μg/mL), spectinomycin (200 μg/mL) and streptomycin (10 μg/mL) were used. In conjugations between *E. coli* and *S. coelicolor*, nalidixic acid (20 μg/mL) was used to counterselect *E. coli*.

Plasmids and primers

All of the plasmids employed in this study are listed in Supplementary Table S3. DNA sequencing was performed by Davis Sequencing (Davis, CA, USA). Supplementary Table S4 shows the primers used in this work, all of which were synthesized by Integrated DNA Technologies. PCR was performed with *Tap* (Invitrogen), *Pfu* (Stratagene, Agilent Technologies), Crimson *Taq* DNA polymerase (New England Biolabs) and Expand High Fidelity PCR system (Roche). All PCR reactions were performed with 5% (vol/vol) DMSO to facilitate amplification of GC-rich DNA (26).

Construction of SCO3084, SCO1308, SCO0266 and SCO3209 null mutants

PCR-targeted mutagenesis was used to replace the *S. coelicolor* SCO3084, SCO0266 and SCO3209 genes with an apramycin resistance cassette, *apr* (27). The requisite PCR products were amplified from the apramycin-resistance gene insert of pIJ773 using primers SCO3084 KO For/SCO3084 KO Rev, and SCO0266 KO For/SCO0266 KO Rev and SCO3209 KO For/SCO3209 KO Rev. The PCR products were individually introduced into *E. coli* BW25113/pIJ790 containing cosmid StE25 (SCO3084) or cosmid 11B10 (SCO0266) or cosmid StE8 (SCO3209) and λ RED recombinase. The resultant recombinant cosmids, StE25 ΔSCO3084::*apr*, 11B10 ΔSCO0266::*apr* and StE8 ΔSCO3209::*apr*, were introduced individually via non-methylating *E. coli* strain ET12567/pUZ8002 into *S. coelicolor* M600 by conjugation as previously described (28). M600 is a plasmid free-derivative of the wild-type strain. Exconjugants lacking the SCO3084, SCO0266 and SCO3209 genes were selected by apramycin resistance and kanamycin sensitivity. Gene replacements were confirmed via PCR on isolated genomic DNA from the null mutants using primers SCO3084 KO Det For/SCO3084 KO Det Rev for *S. coelicolor* B1653 ΔSCO3084::*apr*, and primers

SCO0266 KO Det For/SCO0266 KO Det Rev for *S. coelicolor* B1655 ΔSCO0266::*apr* and primers SCO3209 KO Det For/SCO3209 KO Det Rev for *S coelicolor* B1656 ΔSCO3209::*apr*. The same strategy was used to replace *S. coelicolor* SCO1308 with a spectinomycin cassette (*spec*) in the construction of strain B1654 ΔSCO1308::*spec.* The requisite PCR products were amplified from spectinomycin-resistance cassette from pIJ770 using primers SCO1308 KO For/SCO1308 KO Rev. Recombinant cosmid 5F05 ΔSCO1308::spec was introduced into *S. coelicolor* M600, yielding *S. coelicolor* B1654. Exconjugants were selected by spectinomycin resistance and kanamycin sensitivity. Gene replacements were confirmed via PCR on isolated genomic DNA from the null mutants using primers SCO1308 KO Det For/SCO1308 KO Det Rev.

Complementation of *pobA* (SCO3084) and *pobR* (SCO3209) null mutants

A 1731-bp fragment was excised from cosmid StE25 containing the *pobA* ORF (SCO3084) and 407-bp upstream of its translational start site by restriction digest with BstXI and NcoI. The fragment was treated with DNA polymerase I, Large (Klenow) Fragment (New England Biolabs) according to the manufacturer's protocol. The resulting blunt-ended fragment was ligated into the SmaI site of pBluescript KS+ to yield pJS878. The fragment was then excised from pJS878 with SpeI and EcoRV and ligated into pMS81 pre-treated with the same enzymes to yield pJS880. pMS81 is a site-specific integrating vector that inserts into the ΦBT1 *attB* site of *S. coelicolor* (SCO4848) (29). pJS880 was transformed into non-methylating *E. coli* strain ET12567/pUZ8002 and introduced into *S. coelicolor* via conjugation (28), yielding *S. coelicolor* B1657 ΔSCO3084::*apr* pMS81-SCO3084. Hygromycin-resistant exconjugants were purified by single colony isolation. Phenotypic analyses of *S. coelicolor* B1657 were carried out by growing the strain on media having different carbon sources.

A 1981-bp fragment was excised from cosmid StE8 containing the *pobR* ORF (SCO3209) and 367 upstream base pairs by restriction digest with BlpI and BspEI. The fragment was treated with DNA polymerase I, Large (Klenow) Fragment (New England Biolabs) according to the manufacturer's protocol. The resulting blunt-ended fragment was ligated into the SmaI site of pBluescript KS+ to yield pJS879. The fragment was then excised from pJS879 and ligated into pMS81 as previously described to yield pJS881, which was introduced into the *pobR* null mutant strain *S. coelicolor* B1656 ΔSCO3209::*apr* as previously described. Phenotypic analysis of *S. coelicolor* B1658 was accomplished via RT-PCR analysis of *pobA* (SCO3084).

Assessment of growth on different carbon sources

Strains were cultivated on solid minimal medium containing different carbon sources as described above. In the analyses, confluent lawns each of the four strains of interest (*S. coelicolor* M600*, S. coelicolor* B1653, *S. coelicolor* B1654 and *S.coelicolor* B1657) were grown on Petri dishes containing solid MM media and 2×10^9 spores. Growth was assessed after incubation at 30°C for 10 days.

Transcriptional analyses via RT-PCR

Wild-type *S. coelicolor* M600, ΔSCO0266::*apr*, ΔSCO3209::*apr* and ΔSCO3209::*apr* pMS81-SCO3209 strains were grown as shaken liquid cultures in NMMP for 14 h (mid-exponential phase) after which either PHB, PCA, or ethanol (as a negative control) were added. Both PHB and PCA used in this experiments were dissolved in ethanol. The final concentration of aromatic compounds was 2 mM. After a 1 h induction period, an aliquot of culture sufficient to acquire a cell pellet volume of 100 μL was removed for total mRNA isolation. The cells were washed once with 10.3% (w/v) sucrose solution followed by the addition of 100 μL of 10 mg/mL lysozyme solution (50 mM Tris–HCl, 1 mM EDTA, pH 8.0). The cells were incubated at 37°C for 15 min. Total RNA was isolated using the RNeasy Mini Kit (Qiagen) following the manufacturer's protocol. The concentration of each purified, DNA-free total RNA isolated was measured with a NanoDrop ND-1000 spectrophotometer. An equal amount of total RNA (1200 ng) was used in each RT-PCR. RT-PCR was performed with the OneStep RT-PCR kit (Qiagen) according to the manufacturer's protocol. A 221-bp complementary DNA (cDNA) corresponding to the *pobA* (SCO3084) transcript was detected using primers SCO3084 RT For and SCO3084 RT Rev. A 486-bp cDNA corresponding to the *hrdB* (SCO5820) transcript was detected with *hrdB* RT For/Rev primers in positive control RT-PCR experiments. All primer sequences are listed in Supplementary Table S4. The PCR program used for detection of both transcripts in *S. coelicolor* was: 50°C for 30 min, 95°C for 15 min, 30 cycles of 94°C for 30 s, 56°C for 30 s, and 72°C for 1 min, followed by a final elongation at 72°C for 10 min. The possibility of DNA contamination in the RNA samples was ruled out by using PCR with *Pfu* polymerase under the same conditions. No bands were observed in the controls, indicating that all RT-PCR products correspond to amplification of RNA transcripts.

Mapping of the *pobA* (SCO3084) transcription start site

The transcriptional start sites of *pobA* (SCO3084) were identified with the 5′-RACE System - Rapid Amplification of cDNA Ends, Version 2.0 (Invitrogen). For mapping the *pobA* open reading frame, total RNA was isolated, as previously described, from wild-type *S. coelicolor* M600 grown in NMMP and treated with 2 mM PHB to elevate the level of the *pobA* transcript. The cDNA synthesis was performed using 20 pmol of primer SCO3084 GSP1 and 2000 ng of RNA template according to the manufacturer's protocol for high GC-content transcripts. After cDNA synthesis, the reaction mixture was treated with a RNase Mix to remove template RNA and purified using the S.N.A.P. column procedure. An oligo-dC tail was added to the purified cDNA using the TdT-tailing reaction. Amplification of dC-tailed cDNA was accomplished using a 2.5 μL aliquot of the preceding reaction as template, the primer SCO3084 GSP2 and abridged Anchor primer (AAP, supplied with kit) and *Taq* DNA polymerase. The purified PCR product was then ligated into the pGEM-T Easy vector and transformed into the *E. coli* strain DH5α to yield pJS882. Sequencing of

cloned inserts was performed by Davis Sequencing (Davis, CA, USA).

Gene cloning, protein production, protein purification and size exclusion chromatography

The *pobR* gene (SCO3084; $PobR_{FL}$, residues 1–524) was PCR-amplified from *S. coelicolor* cosmid StE8 and ligated into pBluescript KS+ to yield pJS883. The fragment containing the *pobR* gene was excised and sub-cloned into the RP1B bacterial expression vector (30), which contains an N-terminal His_6-tag and Tobacco Etch Virus (TEV) cleavage site. For expression, the plasmid was transformed into *E. coli* BL21-Gold (DE3) Competent Cells (Agilent). The transformants were inoculated into 50 mL cultures of LB containing 50 μg/mL kanamycin and grown overnight. The resulting cultures were used to inoculate 1 L of LB supplemented with 50 μg/mL kanamycin. After growth at 37°C with vigorous shaking to an OD_{600} between 0.5 and 0.9, the cells were transferred to 4°C for 1 h, treated with 0.5 mM IPTG to induce gene expression, and grown at 18°C for 18 h. The PobR N-terminal (12-267; pJS889) and C-terminal (293-511; pJS890) domains were subcloned into RP1B using identical methods. The expression conditions were the same as described, except that the induced culture of PobR C-terminal domain was grown at 37°C for 4 h.

To purify PobR, the pellet was resuspended in lysis buffer [50 mM Tris pH 8.0, 500 mM NaCl, 0.1% Triton X-100, 5 mM imidazole, Complete tabs-EDTA free (Roche)]. The cells were lysed by high-pressure homogenization using a C3 Emulsiflex high-pressure cell homogenizer (Avestin), and the cell debris was removed by centrifugation (45 000 × *g*/45 min/4°C). The supernatant was filtered through a 0.22-μm membrane (Millipore) and loaded onto a HisTrap HP column (GE Healthcare). His-tagged proteins were eluted using a 5–500 mM imidazole gradient. The fractions containing PobR were identified by SDS-PAGE gel electrophoresis and pooled. The His_6-tag was removed via overnight incubation with TEV protease (dialysis buffer: 20 mM Tris pH 8.0, 500 mM NaCl; 4°C). PobR was further purified using a second Ni-NTA column to separate cleaved protein from the His-tagged protease. The protein was purified in a final step using size exclusion chromatography (SEC; Superdex 75 26/60, GE Healthcare; buffer: 20 mM Tris pH 7.8, 300 mM NaCl, 0.5 mM TCEP, 10% glycerol, 4°C). The PobR:PHB complex was formed by mixing PobR with PHB in a 1:10 ratio, incubating on ice for 1 h, and then purifying the complex using SEC (in SEC buffer).

Agarose electrophoretic mobility shift assays

The 118-bp DNA probe was amplified by PCR using *Pfu* polymerase and the *pobA* promoter For and *pobA* promoter Rev primers. Cosmid StE25 was used as template. The following PCR program was used for amplification: denaturation at 94°C for 3 min, 33 cycles of 94°C for 30 s, 57°C for 30 s and 72°C for 50 s, and a final 10 min elongation at 72°C. PCR products were purified using Qiagen's PCR Purification Kit following the manufacturer's protocol. DNA concentration was determined using a Nanodrop ND-1000 spectrophotometer. Binding of PobR to DNA fragment was performed in 20 μL reaction containing 50 mM Tris–HCl pH 6.0, 50 mM KCl, 5 mM $MgCl_2$, 1 mM EDTA, 10% (vol/vol) glycerol, 0.1 μg poly(dI-dC), 1 mM dithiothreitol (DTT). Each reaction contained 41 nM DNA and between 10 and 500 nM PobR. The effect of aromatic compounds on the binding of PobR to DNA probe was determined by adding the compounds to the pre-formed PobR-DNA reaction mixture. All compounds were dissolved in dimethyl sulfoxide (DMSO). Reactions were incubated at 30°C for 15 min, loaded onto 2% agarose gel and run in Tris-borate EDTA (TBE) buffer at 60 V for 2 h. In experiments where the capacity of aromatic compounds to destabilize the PobR-DNA was assessed, the protein–DNA complexes were treated with the compounds and incubated at 30°C. The samples were then applied to 2% agarose gel and run in Tris-borate EDTA (TBE) buffer at 60 V for 2 h. Gels were subsequently stained with ethidium bromide for visualization of DNA.

DNase I footprinting

For DNase I footprinting, the 118-bp DNA probe was generated as described for the aforementioned agarose EMSAs, except that the 5′ end of primer *pobA* promoter For was labeled with [γ-^{32}P] ATP by T4 polynucleotide kinase (New England Biolabs) following the manufacturer's protocol. Binding of PobR to the DNA fragment was first carried out in a 40 μL reaction volume with 50 mM Tris–HCl pH 6.0, 50 mM KCl, 5 mM $MgCl_2$, 1 mM EDTA and 1 mM dithiothreitol (DTT). The reaction contained 584 nM DNA probe and 4.96 μM PobR. After a 20 min incubation at 30°C, 5 μL of DNase I buffer [100 mM Tris pH 7.6, 25 mM $MgCl_2$, and 5 mM $CaCl_2$] and 0.2 unit of DNase I (New England Biolabs) were added. An additional 2.5 μL of 100 mM $CaCl_2$ were added to the reaction to reduce the amount of free EDTA from the initial PobR–DNA binding reaction that could inhibit the DNAse I activity. The total volume was adjusted to 50 μL with Milli-Q water. The reaction was incubated at 37°C for 5 min and then quenched by the addition of 12 μL 0.1 M EDTA. When the reaction was complete, the DNA was extracted twice with 95 μL of phenol/chloroform/isoamyl alcohol mixture and precipitated with 400 μL 96% ethanol. The resulting pellet was dried under vacuum. In control experiments in which the free DNA duplex was treated with DNAse I, the PobR solution was replaced with an equal volume of the PobR protein storage buffer. Because the enzyme concentration of DNase I optimized for DNase I footprinting resulted in over-cleavage of the free duplex, only 0.08 unit of enzyme DNase I was used and the incubation time was shortened to 1.5 min.

Standard Maxam-Gilbert A/G and C/T reactions were performed on the coding strand of the DNA probe to generate the sequencing markers. The single strand DNA probe was generated by PCR program as described above using 5′-^{32}P end-labeled primer *pobA* promoter For and 118-bp unlabeled double-strand DNA probe as template.

After the DNA pellets were dried, the number of counts was determined in a Perkin-Elmer scintillation counter. After dilution with loading buffer [80% formamide, 10 mM EDTA, 1 mg/ml bromophenol blue and 1 mg/ml xylene

cyanol] to 5000 CMP/μL. 2.1 μL (for DNase I footprinting) and 2.4 μL (for A/G and C/T marker) samples were applied to a 10% denaturing polyacrylamide gel (0.4 mm thick, 59 cm long) and electrophoresed at 80 W. (Electrophoresis was performed until the xylene cyanol dye migrated 7 in.) The gel was dried and used to expose a phosphor-plate for 5 days.

Phosphor-plate was imaged using a Bio-Rad Pharos scanner and the image processing was done using Bio-Rad's Image Lab. First, the gel image was aligned and the lanes were identified. The lane width and position were adjusted, and the position of each band was manually determined. Using the accompanying Maxam-Gilbert sequencing reactions, each band was assigned by nucleotide position and the sequence of PobR binding region was determined.

Crystallization, data collection, and processing

PobR (purified as described above) was concentrated to 6.5 mg/ml, incubated with PHB in 1:10 molar ratio for 1 h, and immediately used for crystallization trials. Crystals were obtained after 7 days at 4°C in 12% PEG MME 2000, 0.1 M MES pH 5.8, 17.5 mM ammonium sulfate using sitting-drop vapor diffusion. Crystals were cryo-protected in mother liquor containing 20% glycerol and frozen in liquid nitrogen. Data for PobR:PHB were collected on a Rigaku FR-E+ SuperBright generator using a Saturn 944G CCD detector. Diffraction data were processed to 2.06 Å using HKL3000 (31). The *Rhodococcus jostii* RHA1 RHA06195 (PDB: 2IA2) structure was identified by the Fold and Function Assignment Server as a suitable initial molecular replacement (MR) model (-71.2 score, 46% sequence identity) (32). Chainsaw (33) was used create a polyalanine model of domain A of 2IA2 which was then used for molecular replacement using Phaser (34). Iterative model building and refinement were performed using COOT (35) and PHENIX (36). MOLPROBITY was used for model validation (37). Data collection and structure refinement statistics are reported in Table 1.

Isothermal titration calorimetry

Isothermal titration calorimetry (ITC) experiments were performed using a VP-ITC (GE Healthcare) at 25°C. Ligands were dissolved in ITC assay buffer (20 mM Tris pH 7.8, 300 mM NaCl, 0.5 mM TCEP, 10% glycerol), and both protein and ligand were degassed under vacuum. Ligands (600 μM PHB, 1.2 mM 2,4-dihydroxybenzoate) were titrated (10 μL injections every 300 s, 35 times) into the cell containing 60 μM monomeric PobR under constant stirring (307 rpm). Titration of the ligand into buffer resulted in a negligible heat of dilution for each ligand. Data were analyzed using NITPIC (38) and SEDPHAT (39).

RESULTS AND DISCUSSION

S. coelicolor has a *pobA* gene (SCO3084) encoding *p*-hydroxybenzoate hydroxylase

Bioinformatic analyses of the *S. coelicolor* genome sequence revealed two genes (SCO1308 and SCO3084) predicted to encode enzymes that are homologous to *p*-hydroxybenzoate hydroxylase from *P. fluorescens* and *P. aeruginosa* (40,41) (http://streptomyces.org.uk). To test the functional predictions, PCR-targeting was used to construct SCO3084 (*S. coelicolor* B1653 ΔSCO3084::*apr*) and a SCO1308 (*S. coelicolor* B1654 ΔSCO1308::*spec*) null mutants in which the genes were replaced with genetic markers for resistance to apramycin and spectinomycin, respectively.

It was found that the SCO3084 null mutant was unable to grow on solid media having PHB as the primary carbon source. Importantly, like the wild-type strain, the null mutant retained the capacity to grow on media with PCA (the product of PHB hydroxylation) as the primary carbon source. In contrast, there was no significant difference in growth between wild-type *S. coelicolor* and the SCO1308 null strain on media with either PHB or PCA (Figure 1). These observations suggested that only SCO3084 encodes a functional *para*-hydroxybenzoate hydroxylase. Our finding that provision of SCO3084 under the control of its native promoter to the SCO3084 null strain restored growth on media with PHB indicated that the gene was necessary and sufficient for PHB catabolism (Supplementary Figure S1).

To further establish that SCO3084 encodes a functional *para*-hydroxybenzoate hydroxylase, we biochemically characterized its product. We subcloned the presumptive *pobA* gene (SCO3084) with an N-terminal His_6 affinity tag, het-

Table 1. Data collection and refinement statistics

	PobR:PHB[a]
Protein	
PDBID	5W1E
Data collection	
Space group	$P2_1$
Cell dimensions	
a, *b*, *c* (Å)	44.1, 87.9, 69.9
α, β, γ (°)	90.0, 96.2, 90.0
Resolution (Å)	50.0–2.06 (2.10–2.06)*
R_{merge}	33.0 (8.8)
$I/\sigma I$	26.6 (4.8)
Completeness (%)	99.7 (95.6)
Redundancy	7.3 (5.3)
Refinement	
Resolution (Å)	32.32–2.06 (2.12–2.06)
No. reflections	32696
R_{work}/R_{free}	0.164 (0.206)/0.189 (0.242)
No. atoms	
Protein	3725
Glycerol/SO_4	17
PHB	10
Water	383
B-factors	
Protein	26.4
Glycerol/SO_4	40.5
PHB	20.4
Water	34.7
RMS deviations	
Bond lengths (Å)	0.002
Bond angles (°)	0.548
Ramachandran	
Outliers (%)	0.0
Allowed (%)	1.6
Favored (%)	98.4
Clashscore	2.38

Data were collected from a single crystal.
Values in parentheses are for highest-resolution shell.

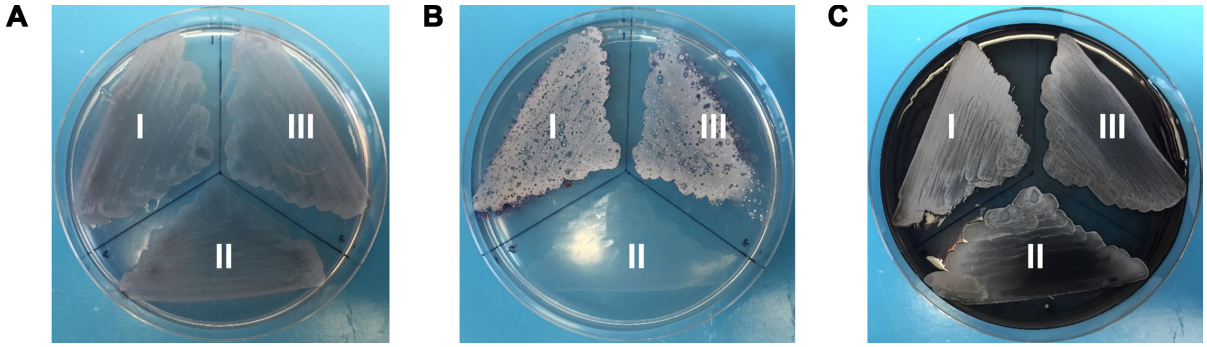

Figure 1. Carbon source utilizations of wild-type *S. coelicolor* M600 (I), *S. coelicolor* B1653 (ΔSCO3084::*apr*) (II), and *S. coelicolor* B1654 (ΔSCO1308::*spec*) (III). SCO1308 and SCO3084 encode two homologs of *para*-hydroxybenzoate hydroxylase. The strains were grown for 10 days at 30°C on MM media solidified by Gelzan and having different carbon sources. From left to right, (**A**) 0.5% (w/v) glucose, (**B**) 20 mM PHB, and (**C**) 20 mM PCA. Deletion of SCO3084 in *S. coelicolor* only abolished its ability to grow on plates having PHB as the primary carbon source, whereas disruption of SCO1308 did not affect the bacterium's growth on PHB, PCA, or glucose.

erologously expressed it in *E. coli*, and purified the gene product to homogeneity using metal-affinity chromatography (Supplementary Figure S2A). The purified protein exhibited the characteristic spectroscopic properties of a flavin-dependent enzyme (*i.e.*, absorbance maxima at 370 and 450 nm) (Supplementary Figure S2B). The conversion of PHB to PCA in buffer (Tris–HCl, pH 7.4) containing the purified protein and the co-factors FAD and NADPH (19), proved that it is a *para*-hydroxybenzoate hydroxylase (Supplementary Figure S2C).

Transcription of the gene *pobA* is induced by PHB and its analogs

PHB has been reported to induce transcription of *pobA* in *Acinetobacter calcoaceticus* (22,23). To determine if the transcription of *pobA* in *S. coelicolor* is induced by PHB, semi-quantitative reverse transcription polymerase chain reaction (RT-PCR) was performed. Figure 2A shows that *pobA* was robustly transcribed when *S. coelicolor* was grown in liquid media supplemented with PHB, whereas only a basal level of transcription was observed when the bacterium was grown in media lacking PHB. Interestingly, we found that PHB analogs, including 2,4-dihydroxybenzoate (2,4-DHB) and protocatechuic acid (PCA, the product of PobA catalyzed hydroxylation) also induce the transcription of *pobA*. These observations differ from studies in *A. calcoaceticus* wherein only PHB induces the transcription of *pobA* (22).

Transcription of the gene *pobA* is negatively regulated by SCO3209 (*pobR*)

Based on the regulated transcription of *pobA,* we sought to identify the cognate transcriptional regulator. In *A. calcoaceticus,* expression of *pobA* is regulated by PobR, which is a transcriptional activator (22,23). Thus, we searched for *pobR* homologs in the *S. coelicolor* genome. Unexpectedly, no homologs of *pobR* were found in close proximity to SCO3084. A BLASTp analysis (42) identified gene candidates encoding regulators that are homologous to PobR. The closest homolog was gene SCO3209, whose product shares 35% identity with PobR from *A. calcoaceticus.* Additionally, analysis of *S. coelicolor* genome functional annotations also revealed that SCO0266 encodes a putative regulator that is 30.3% identical to PobR from *Pseudomonas sp.* strain HR199. To determine if either or both of the two genes regulates the transcription of *pobA*, we performed PCR-targeted gene replacement to construct SCO3209 (*S. coelicolor* B1656 ΔSCO3209::*apr*) and SCO0266 (*S. coelicolor* B1655 ΔSCO0266::*apr*) null strains. Interestingly, the gene *pobA* (SCO3084) was constitutively transcribed in the SCO3209 null mutant in the absence and presence of PHB. In contrast, deleting gene SCO0266 did not affect the *pobA* transcription (Figure 2B). The SCO3209 null mutant's defect in *pobA* transcription was suppressed by complementation (Figure 2C). These data show that SCO3209 encodes a repressor of *pobA* gene transcription, which we named its product PobR.

S. *coelicolor* PobR is a translational fusion of two IclR family proteins

Strikingly, SCO3209 is predicted to encode a 55-kDa protein that is roughly twice the size of canonical IclR transcription factors. Using HMMER (43) and protein BLAST (42), we determined that *S. coelicolor* PobR has N- and C-terminal domains that each exhibit homology with IclR family transcription factors (Figure 3A; the two domains of PobR were also predicted to be structurally similar by FFAS (32,44)). With respect to its domain organization, PobR is atypical among IclR family members and transcription factors in general. Protein BLAST analyses (Supplementary Table S5) against streptomycete genomes in the IMG (Integrated Microbial Genomes) database showed that this peculiar PobR is highly conserved (Supplementary Figure S3).

Heterologous expression of the full-length *pobR* gene in *E. coli* yielded a soluble product of the expected size (Supplementary Figure S4A). Unlike the construct corresponding to the full length PobR, heterologous expression of the individual domains in *E. coli* did not yield soluble protein. Furthermore, we found that expression of the individual domains in wild-type *S. coelicolor* did not interfere with repression of *pobA* transcription and that their expression in

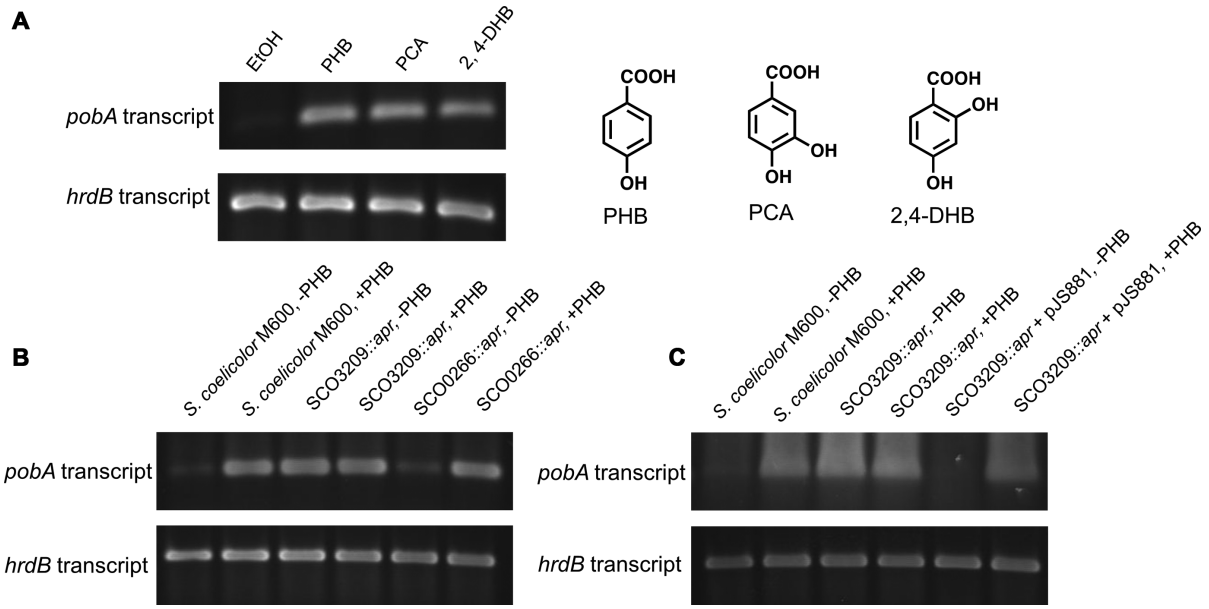

Figure 2. Transcriptional analyses of *pobA* (SCO3084). (**A**) RT-PCR was used to detect the *pobA* transcript when *S. coelicolor* is grown in NMMP media supplemented with solutions of PHB, PCA, or 2,4-dihydroxybenzoate (2,4-DHB) dissolved in ethanol. PHB and PCA are the substrate of PobA and product of the PobA-catalyzed reaction, respectively. 2,4-DHB is an isomer of PCA. A positive control, the transcript of the constitutive *hrdB* gene, was detected in all of the RNA samples (26). All compounds induced transcription of *pobA*. (**B**) RT-PCR was used to detect the transcription of *pobA* in wild-type *S. coelicolor* and the SCO0266 or SCO3209 null strains grown in liquid NMMP medium. *hrdB* was used as a positive control. Only disruption of SCO3209 affected PHB-dependent transcription of *pobA*. (**C**) RT-PCR was used to detect the transcription of *pobA* in the SCO3209 null strain having a plasmid with the cognate wild-type locus grown (pJS881) in liquid NMMP medium. The SCO3209 null strain's defect in *pobA* transcription was suppressed by provision of pJS881. SCO3209 (*pobR*) encodes a negative, PHB-dependent regulator of the *pobA* gene.

the *pobR* null strain did not restore repression of *pobA* transcription (Supplementary Figure S4B).

PobR binds an imperfect inverted repeat sequence in the *pobA* promoter region

Our genetic and transcriptional analyses suggested that SCO3209 encodes a transcriptional repressor that is functionally affected by PHB. Most IclR regulators repress transcription by binding a specific DNA sequence (usually an inverted repeat) that overlaps with the RNA polymerase binding site. We thus predicted that PobR represses the transcription of *pobA* via a similar mechanism. To test this prediction, we used 5′ rapid amplification of cDNA ends (5′-RACE) experiments to map the transcription start site of the *pobA* gene. The transcription of *pobA* was mapped to two sites, 109 and 110 bp upstream of the *pobA* translation start site (–109 and –110) (Figure 3B). The putative –10 and –35 sites of the promoter were assigned on the basis of congruence with a consensus sequence among streptomycete promoters (45). Next, electrophoretic mobility shift assays (EMSAs) were used to assess the binding of PobR to *pobA* promoter region. A 118-bp PCR-amplified fragment spanning the entire region between the predicted promoter and the *pobA* open reading frame start codon (ATG) was used as the DNA probe in EMSAs. As shown in Figure 3C, increasing quantities of purified PobR shifted the migration of the DNA probe. In order to identify the DNA sequence of the binding region, we performed DNase I footprinting. The same 118-bp DNA segment labeled at 5′ end with [γ-^{32}P] ATP was treated with DNase I in the presence and absence of purified PobR. As shown in Figure 3D, a single region adjacent to the putative transcriptional promoter of *pobA* was protected from nuclease digestion. The 30-bp site protected by PobR is an imperfect, inverted repeat sequence. As there was only one shifted protein-DNA complex in the EMSAs and only one sequence was protected by PobR, we concluded that there is only one operator for protein binding in the *pobA* upstream region. Subsequent sequence alignments (ClustalX2) (46) of the *pobA* upstream regions (up to –150 bp nucleotide) and Gibbs motif sampler analysis (47) showed that PobR binding site sequences are conserved in multiple *Streptomyces* species (Figure 3E).

PHB binds directly to PobR and destabilizes DNA binding

IclR family repressors typically regulate transcription through ligand-mediated changes in oligomerization state that can affect DNA binding (48,49). In the absence of ligand, they form tetramers that are competent for DNA binding; whereas, the ligand favors a dimeric state that is unable to bind DNA. Because *pobA* transcription was regulated by PobR and also induced by PHB, we hypothesized that PHB is the ligand of PobR and that its binding to the transcriptional repressor would attenuate binding to the operator of *pobA* via induced changes in oligomerization state. To test this, we used electrophoretic mobility shift assays (EMSAs). The data showed that pre-formed PobR-DNA complexes were destabilized upon treatment with PHB (Figure 4A), as we predicted. Interestingly, in addition the ligand-dependent attenuation of DNA binding, we observed a species in the EMSAs having a mobility

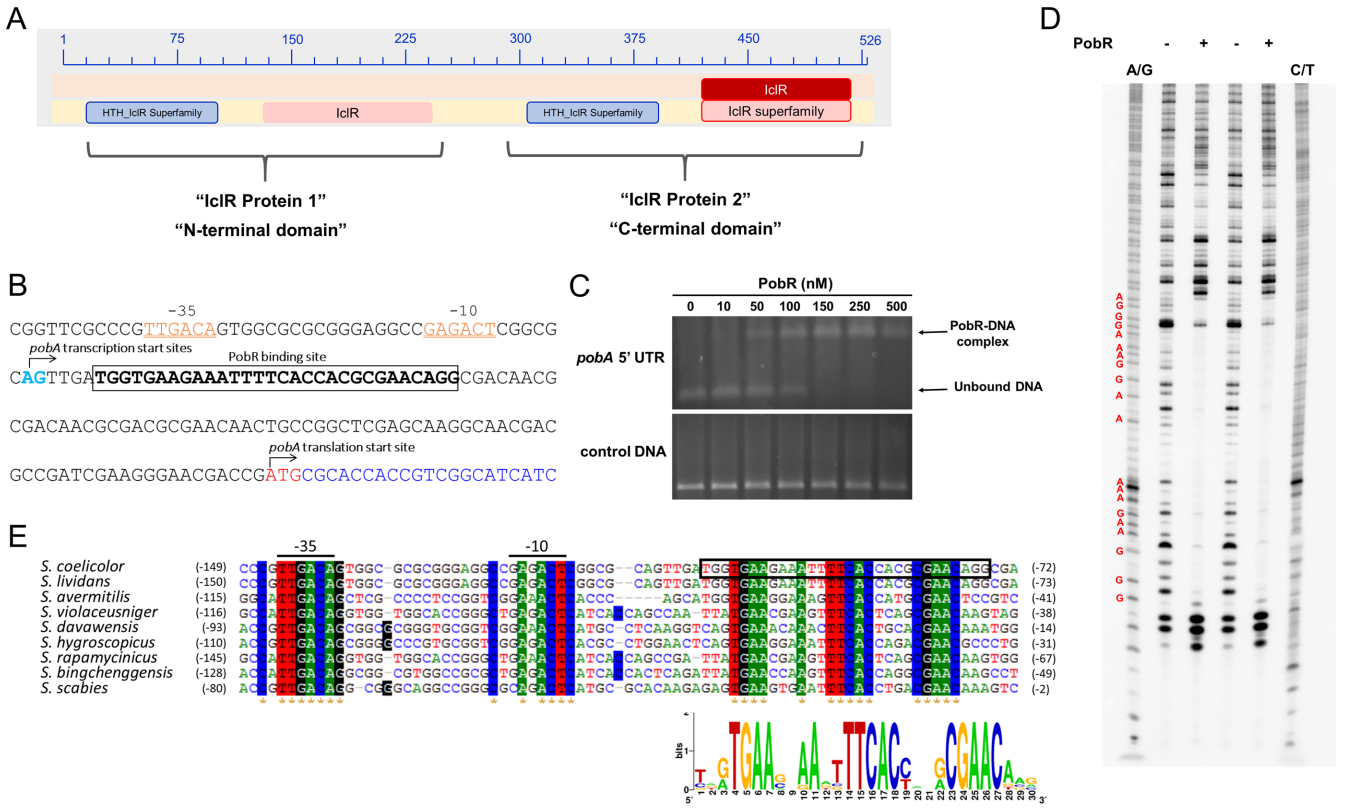

Figure 3. Biochemical and bioinformatic analyses of PobR, a negative regulator of *pobA*. (**A**) Predicted domains organization of PobR protein. Both N-terminal domain and C-terminal domains of PobR are homologous to intact IclR family transcription factors. (**B**) The overall view of the region upstream of the *pobA* open reading frame (ORF), highlighting the transcription start site of *pobA* (turquoise), putative -35 and -10 *pobA* promoter elements (underlined and highlighted in orange) and the PobR regulator binding site sequence (in bold and boxed). (**C**) DNA binding of PobR was assessed using agarose electrophoretic mobility shift assays (EMSAs). A PCR-amplified DNA fragment spanning the entire region between the transcription and translation start sites (5′-untranslated region) was titrated with PobR. In comparison with the unbound DNA probe in the electrophoresis, retarded migration of the DNA probe was observed upon addition of PobR. Bands representing the PobR-DNA probe complex and the unbound DNA probe are highlighted by arrows. For a negative control, a 486-bp fragment amplified from *hrdB* ORF, which does not contain the PobR binding site, was used. (**D**) The PobR binding site upstream of the *pobA* ORF was mapped using DNase I footprinting analysis. A 5′-^{32}P end-labeled 118-bp DNA fragment was digested with DNase I in the absence and presence of heterologously produced and purified PobR. In comparison with the DNA digest in the absence of PobR, a protected region was observed when DNA was incubated with PobR before digestion. Sequencing ladders indicated by lanes C/T and A/G were generated via Maxam-Gilbert reactions. The reactions were performed in duplicate. (**E**) Sequence alignment of the regions upstream of the *pobA* ORFs in various streptomycetes. Putative –35 and –10 *pobA* promoter elements and PobR binding site sequence (boxed) identified in DNase I footprinting reaction are conserved in several members of the *Streptomyces* genus. A conserved PobR binding site was also identified using the Gibbs Motif Sampler (47). Sequence logo images (51) depict the sequence conservation of PobR binding site.

slightly more than that of the PobR–DNA complex (Figure 4A). Though its identity and significance are not obvious, we assume that it reflects a distinct complex of the protein and DNA. Nevertheless, we then used size exclusion chromatography (SEC) to determine if PHB binding to PobR results in a change in the PobR oligomerization state. The data show that PobR, which is predicted to contain two IclR domains, is dimeric in the absence of PHB, yet monomeric in its presence (Figure 4B). Despite its unusual structure, *S. coelicolor* PobR behaves in a similar fashion to other IclR family transcriptional repressors with respect ligand-induced changes in oligomerization state and DNA affinity. These observations were confirmed using SAXS (Supplementary Figure S5).

To gain additional insights into binding of PHB to PobR, we assessed affinity in the protein ligand interaction using isothermal calorimetry. The data show that PHB binds directly to PobR with a dissociation constant (K_D) of 5.8 ± 0.5 μM (Figure 4C), a value comparable to those observed between other IclR proteins and their corresponding ligands (50). Curiously, the data also revealed that PHB binds PobR in a 1:1 ratio, and not the expected 2:1 ratio. Thus, we predicted that only one of the two ligand binding domains in PobR is competent to bind PHB.

The PobR-PHB structure shows that PobR contains two IclR domains but that both have features that are distinct from the canonical IclR family

To determine why PobR binds only one molecule of PHB, we determined the crystal structure of the PobR:PHB complex to 2.06 Å (data collection and refinement statistics are provided in Table 1). As predicted, PobR is composed of two IclR domains (Figures 5A and B), IclR1 and IclR2, which are each composed of a DNA binding domain (DBD; DBD1 and DBD2; also known as a winged HTH domain (wHTH) and a ligand/effector binding domain (LBD;

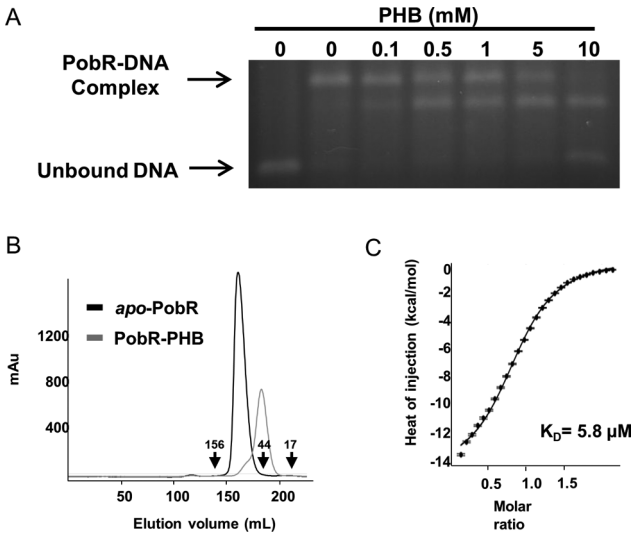

Figure 4. PHB attenuates DNA binding by PobR and affects the protein's oligomerization state. (**A**) A PobR-DNA complex was titrated with PHB in agarose EMSAs. The dissociation of PobR from the DNA probe was observed upon the addition of increasing amounts of PHB. Unbound DNA was used as control in the first lane. (**B**) Size exclusion chromatography elution profiles of *apo*-PobR (black) and the PobR-PHB complex (gray). The predicted molecular weight for a PobR dimer is 110 kDa, whereas that of a monomer is 55 kDa. Elution positions of MW standards are indicated by arrows and labeled as 156, 44 and 17 kDa. (**C**) Isothermal calorimetry was used to assess the binding of PHB to *apo*-PobR and to assess the dissociation constant. The binding isotherm of PobR with PHB is shown and the calculated dissociation constant (K_D) is 5.8 μM.

LBD1 and LBD2). A linker connects the two IclR domains (^{272}PAPEPGPPPAGLALWTGASKQELGREF^{298}). The two IclR domains adopt different conformations, due to hinge rotation at a single residue (Arg90; Ser374) that connect the DBDs to the LBDs. The final structure includes residues 12–524 (with the exception of aa 415–427, which was not modeled as it lacked electron density).

The two DBDs form a tight complex and are related by a pseudo two-fold axis (Figure 5A). Based on the structures of other IclR proteins, the predicted function of helix α3 from both domains is binding in the major grooves of the promoter DNA (Figure 5D). The DBDs are not identical, as their superposition revealed a root mean square deviation (RMSD) of 0.78 Å. The largest difference is in the 'wing' of the wHTH domain, with the beta hairpin (β1–β2) of DBD2 being one residue longer than the corresponding region in DBD1. An additional element in the DBDs is the linker that connects the two IclR domains (Figure 5A, green). It forms an additional helix that is 'wedged' between DBD1 and DBD2 and thus may also contribute to DNA binding.

The PobR effector (or ligand) binding domains are comprised of a six-stranded β-sheet sandwiched by either 5 (LBD1) or 4 (LBD2) α-helices. A sequence-based alignment of IclR1 and IclR2 with the most similar IclR proteins whose structures are known (Supplementary Figure S6) show that both PobR LBDs have features that make it unique from other IclR domains. Namely, LBD1 has an insert between helices α7 and α8, while LBD2 is missing helix α7 altogether.

Only the PobR N-terminal IclR domain is competent to bind PHB

The PobR:PHB complex reveals that only LBD1 binds PHB, consistent with the ITC data that showed that PHB binds PobR with a 1:1 molar ratio (Figure 4C). PHB binds in a deep hydrophobic pocket at the cleft of the twisted β-sheet that is covered by long loops (Figure 5E). Ligand binding is stabilized by both electrostatic and hydrophobic interactions. In the former, the PHB's hydroxyl is engaged in salt bridge and hydrogen bonding interactions with side chains of Gln125, Arg130 and Asp208 and with the backbone amide of Ala148 (Figure 6A). In the latter, the PHB aromatic moiety also exhibits hydrophobic interactions with Phe122, Phe136, Ala218 and Val238 (Figure 6A).

Superposition of LBD1 and LBD2 suggests why only LBD1 binds PHB. It is apparent that LBD2 is missing cognate residues of LBD1 that are ordered and engaged with PHB. For example, the extended loop with ligand interacting residues 160–190 in LBD1 (Figure 5E) is not present in LBD2. Further, the residues that correspond to Arg130 (two salt bridge interactions) and Phe136 (hydrophobic contacts) are missing entirely in LBD2, as no electron density was observed for the loop in which these corresponding residues are located. Additionally, LBD2 has a hydrophobic valine residue (Val453) in place of LBD1's Asp208, which hydrogen bonds with the hydroxyl group of PHB (Figure 6B). While the aforementioned cases reflect missing residues, we also note that residues 415–427 within LBD2 could not be modeled due to a lack of density suggesting that these residues are flexible and may lack the order required for ligand binding. The corresponding residues of LBD1 are ordered and have key contacts with PHB (Figure 5E).

CONCLUSIONS

We have characterized the catabolism of the lignin-derived aromatic compound PHB and its regulation in *S. coelicolor*. Our efforts began with bioinformatic analyses of the *S. coelicolor* genome that suggested genetic and functional redundancies in these phenomena. Specifically, there were two *pobA* gene homologs encoding putative *para*-hydroxybenzoate hydroxylase (SCO1308 and SCO3084) and two genes encoding homologs of the PobR transcription factors known to regulate *pobA* transcription (SCO0266 and SCO3209). Surprisingly, genetic analyses indicated that only one member of each pair was functionally related to PHB catabolism. Further work is required to assign the functions of the other *pobA* and *pobR* orthologs. In any case, we identified a single *para*-hydroxybenzoate hydroxylase (SCO3084) that is active in PHB catabolism. Unexpectedly, we also discovered that the transcriptional regulator that regulates *pobA* (SCO3209) is a unique protein amongst the predicted 7825 proteins in *S. coelicolor* (41) because it is a translational fusion of two IclR family transcription factors. Each domain (N-terminal domain and C-terminal domain) is structurally similar to an intact IclR family protein. Curiously, sequence alignment indicated that there is no nucleotide sequence similarity between the two DNA fragments encoding N-terminal domain and C-terminal domain. The amino acid sequence similarity of

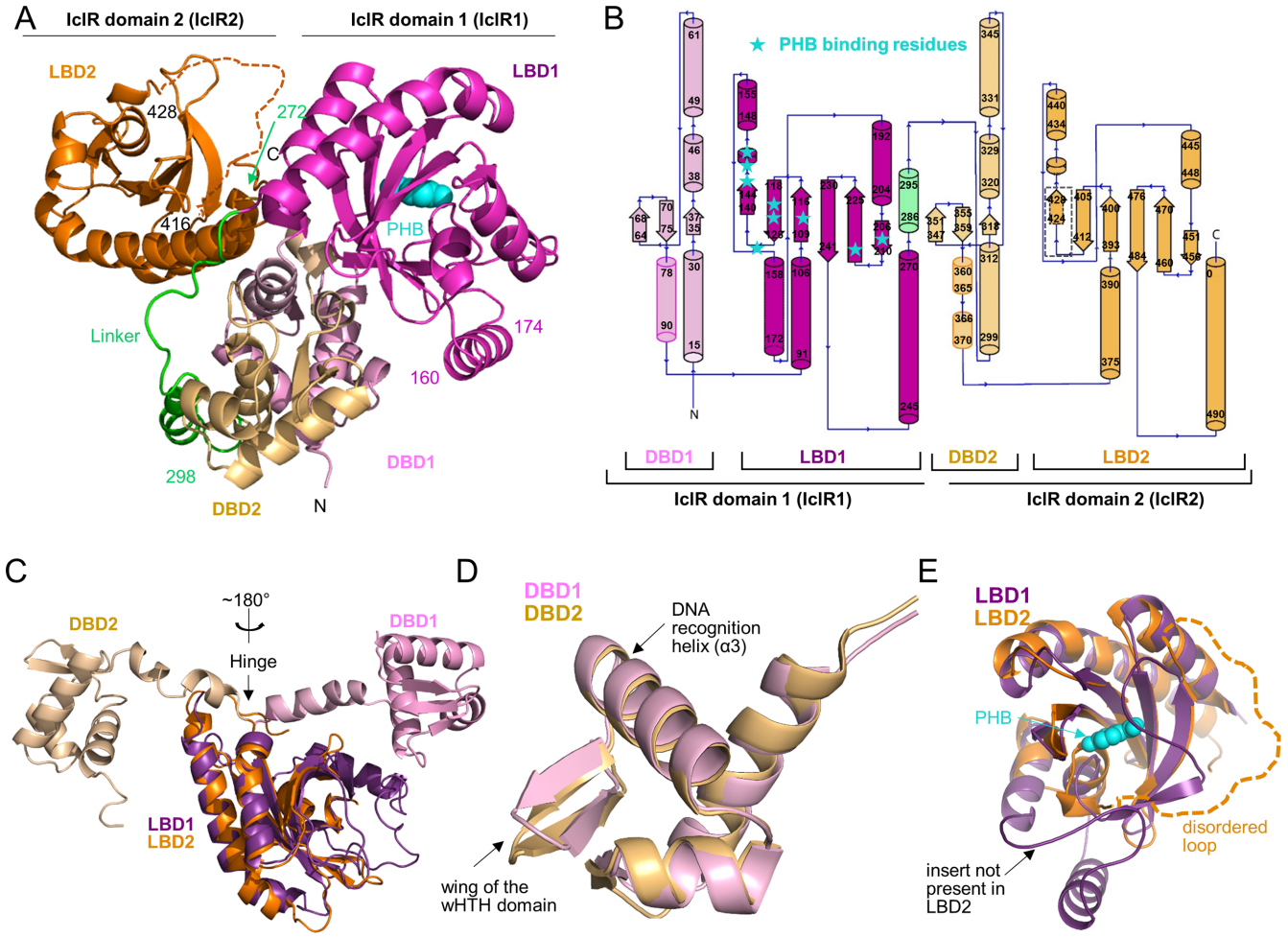

Figure 5. PobR contains two IclR domains, only one of which binds PHB ligand. (**A**) Ribbon diagram of the PobR-PHB complex. IclR domain 1 (IclR1) is pink/violet while IlcR domain 2 (IclR2) is beige/orange. Each IclR domain consists of a DNA binding domain (DBD1, pink; DBD2, beige) and a ligand binding domain (LBD1, violet; LBD2, orange). They are connected by a ∼25 residue linker (aa 272–298; green). LBD1 has a helix not present in LBD2 (α-helix insert) and 12 residues of LBD2 were not visible in the electron density map and thus not modelled (orange dashed line). One molecule of PHB (cyan spheres) is bound to LBD1. (**B**) Secondary structure topology diagram of the PobR-PHB complex; colors as in (A). Blue stars indicate residues that mediate PHB binding; the hinge about which the LBD and DBD domains rotate with respect to one another is indicated by an arrow. (**C**) Overlay of the IclR1 and IclR2 domains using the LBDs for the superposition; colors as in (A). (**D**) Superposition of DBD1 and DBD2; colors as in (A). (**E**) Superposition of LBD1 and LBD2; colors as in (A).

the two domains is also low with an identity of only 44%. Arguably, the alignments indicate that a gene duplication event cannot be invoked to explain for the origins of *pobR* gene. It is more likely that the peculiar organization of the *pobR* gene is the product of gene excision and re-assembly during evolution. These genetic events were likely recent because PobR is only observed and conserved in members of the *Streptomyces* genus as shown in Supplementary Table S5. However, the reasons why PobR has the unique structural organization and why it is only conserved in *Streptomyces* genus are unclear.

PobR is also noteworthy because it is the only IclR family transcription factor that functions as a repressor in the degradation of aromatic compounds (15). Our crystal structure of PobR in complex with its effector ligand is the first structure of a full-length IclR family transcription factor in complex with an effector ligand. Because of its unique organization (two fused IclR domains), only one LBD is capable of binding directly to ligand, PHB. In addition, because *S. coelicolor* PobR cannot bind DNA in the presence of PHB, it could be argued that the monomeric structure has a conformation that precludes DNA binding its helix-turn-helix domains. Unfortunately, while the SAXS analysis confirms the dimeric structure of PobR in the absence of ligand, it does not have the resolution to clarify the means by which it binds DNA.

Overall, this work provides novel insights into the molecular mechanisms of IclR family transcriptional repressors in aromatic catabolism and the structures of IclR family members. These studies of aromatic catabolism open the door to the exploitation of microorganisms for the conversion of aromatic compounds to commodity chemicals and biofuels.

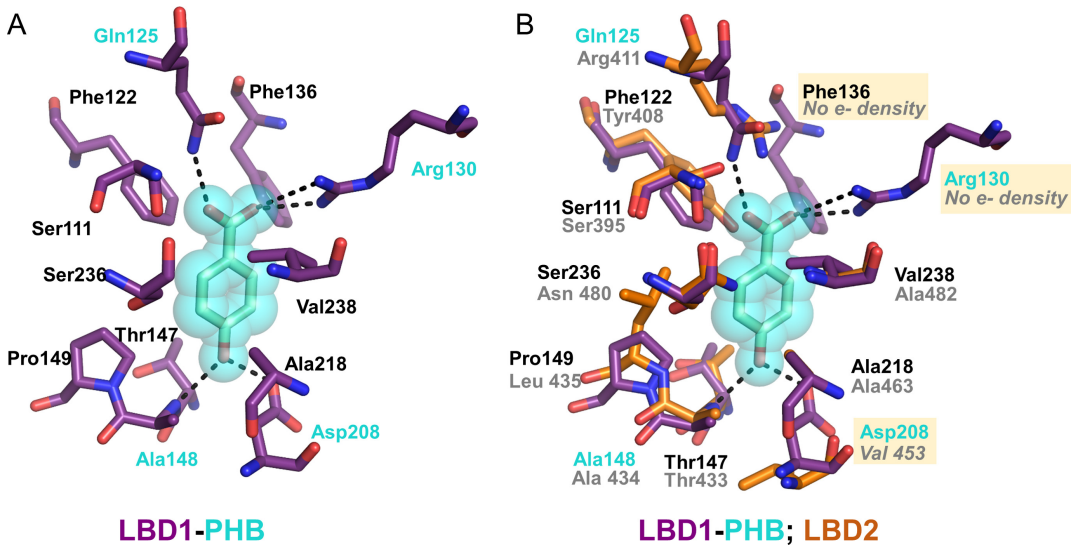

Figure 6. PHB binds PobR via electrostatic and hydrophobic interactions. (**A**) PHB (cyan) binding pocket in LBD1. Electrostatic interactions indicated by black dashed lines and the residues labelled in cyan. (**B**) Same as (A), but with LBD2 superimposed on LBD1 and the corresponding LBD2 residues shown as sticks. Missing interactions between residues in LBD2 are indicated by a beige square.

AVAILABILITY

The structure factors and coordinates have been deposited in the PDB under accession number 5W1E.

SUPPLEMENTARY DATA

Supplementary Data are available at NAR online.

FUNDING

NSF CAREER awards [MCB1053319 to J.K.S. and MCB0952550 to R.P.]; Crystallographic data was obtained at the Brown University Structural Biology Core Facility; Seed award from the Office of Vice President for Research at Brown University (to J.K.S. and R.P.). Funding for open access charge: Brown University and the University of Arizona.
Conflict of interest statement. None declared.

REFERENCES

1. Adler,E. (1977) Lignin chemistry—past, present and future. *Wood Sci. Technol.*, **11**, 169–218.
2. Rubin,E.M. (2008) Genomics of cellulosic biofuels. *Nature*, **454**, 841–845.
3. Weng,J.K., Li,X., Bonawitz,N.D. and Chapple,C. (2008) Emerging strategies of lignin engineering and degradation for cellulosic biofuel production. *Curr. Opin. Biotechnol.*, **19**, 166–172.
4. Chundawat,S.P., Beckham,G.T., Himmel,M.E. and Dale,B.E. (2011) Deconstruction of lignocellulosic biomass to fuels and chemicals. *Annu. Rev. Chem. Biomol. Eng.*, **2**, 121–145.
5. Dean,B.J. (1985) Recent findings on the genetic toxicology of benzene, toluene, xylenes and phenols. *Mut. Res./Rev. Genet. Toxicol.*, **154**, 153–181.
6. Fuchs,G., Boll,M. and Heider,J. (2011) Microbial degradation of aromatic compounds - from one strategy to four. *Nat. Rev. Microbiol.*, **9**, 803–816.
7. Haggblom,M.M. and Milligan,P.W. (2000) Anaerobic biosdegradation of halogenated pesticides: influence of alternate electron acceptors. *Soil Biochem. (Marcel Dekker, Inc. New York)*, **10**, 1–22.
8. Ornston,L.N. and Parke,D. (1977) The evolution of induction mechanisms in bacteria: insights derived from the study of the beta-ketoadipate pathway. *Curr. Top. Cell Regul.*, **12**, 209–262.
9. Harwood,C.S. and Parales,R.E. (1996) The beta-ketoadipate pathway and the biology of self-identity. *Annu. Rev. Microbiol.*, **50**, 553–590.
10. Kamimura,N. and Masai,E. (2014) The protocatechuate 4,5-cleavage pathway: overview and new findings. *Biodegradative Bacteria*. pp. 207–226.
11. Crawford,R.L. (1975) Novel pathway for degradation of protocatechuic acid in *Bacillus* species. *J. Bacteriol.*, **121**, 531–536.
12. Crawford,R.L., Bromley,J.W. and Perkins-Olson,P.E. (1979) Catabolism of protocatechuate by *Bacillus macerans*. *Appl. Environ. Microbiol.*, **37**, 614–618.
13. Kasai,D., Fujinami,T., Abe,T., Mase,K., Katayama,Y., Fukuda,M. and Masai,E. (2009) Uncovering the protocatechuate 2,3-cleavage pathway genes. *J. Bacteriol.*, **191**, 6758–6768.
14. Masai,E., Katayama,Y. and Fukuda,M. (2007) Genetic and biochemical investigations on bacterial catabolic pathways for lignin-derived aromatic compounds. *Biosci. Biotechnol. Biochem.*, **71**, 1–15.
15. Díaz,E. and Prieto,M.A.A. (2000) Bacterial promoters triggering biodegradation of aromatic pollutants. *Curr. Opin. Biotechnol.*, **11**, 467–475.
16. Lorenzo,V. and Pérez-Martín,J. (1996) Regulatory noise in prokaryotic promoters: how bacteria learn to respond to novel environmental signals. *Mol. Microbiol.*, **19**, 1177–1184.
17. Davis,J.R. and Sello,J.K. (2010) Regulation of genes in *Streptomyces* bacteria required for catabolism of lignin-derived aromatic compounds. *Appl. Microbiol. Biotechnol.*, **86**, 921–929.
18. Davis,J.R., Brown,B.L., Page,R. and Sello,J.K. (2013) Study of PcaV from *Streptomycescoelicolor* yields new insights into ligand-responsive MarR family transcription factors. *Nucleic Acids Res.*, **41**, 3888–3900.
19. Paul,D., Chauhan,A., Pandey,G. and Jain,R.K. (2004) Degradation of *p*-hydroxybenzoate via protocatechuate in *Arthrobacter protophormiae* RKJ100 and *Burkholderia cepacia* RKJ200. *Curr. Sci. India*, **87**, 1263–1268.
20. Hosokawa,K. and Stanier,R.Y. (1966) Crystallization and properties of *p*-hydroxybenzoate hydroxylase from *Pseudomonas putida*. *J. Biol. Chem.*, **241**, 2453–2460.
21. Howell,L.G., Spector,T. and Massey,V. (1972) Purification and properties of *p*-hydroxybenzoate hydroxylase from *Pseudomonas fluorescens*. *J. Biol. Chem.*, **247**, 4340–4350.
22. DiMarco,A.A., Averhoff,B. and Ornston,L.N. (1993) Identification of the transcriptional activator *pobR* and characterization of its role in the expression of pobA, the structural gene for *p*-hydroxybenzoate

hydroxylase in *Acinetobacter calcoaceticus*. *J. Bacteriol.*, **175**, 4499–4506.
23. DiMarco,A.A. and Ornston,L.N. (1994) Regulation of *p*-hydroxybenzoate hydroxylase synthesis by PobR bound to an operator in *Acinetobacter calcoaceticus*. *J. Bacteriol.*, **176**, 4277–4284.
24. Bertani,I., Kojic,M. and Venturi,V. (2001) Regulation of the *p*-hydroxybenzoic acid hydroxylase gene (*pobA*) in plant-growth-promoting *Pseudomonas putida* WCS358. *Microbiology*, **147**, 1611–1620.
25. Sambrook,J., Fritsch,E.F. and Maniatis,T. (1989) *Molecular Cloning: A Laboratory Manula*. 2nd edn, Cold Spring Harbor Laboratory Press, NY.
26. Kieser,T., Bibb,M.J., Buttner,M.J., Chater,K.F. and Hopwood,D.A. (2000) *Practical Streptomyces Genetics*. John Innes Foundation, Norwich.
27. Gust,B., Challis,G.L., Fowler,K., Kieser,T. and Chater,K.F. (2003) PCR-targeted *Streptomyces* gene replacement identifies a protein domain needed for biosynthesis of the sesquiterpene soil odor geosmin. *Proc. Natl. Acad. Sci. U.S.A.*, **100**, 1541–1546.
28. Jones,G.H., Paget,M.S.B., Chamberlin,L. and Buttner,M.J. (1997) Sigma-E is required for the production of the antibiotic actinomycin in *Streptomyces* antibioticus. *Mol. Microbiol.*, **23**, 169–178.
29. Gregory,M.A., Till,R. and Smith,M.C.M. (2003) Integration site for *Streptomyces* phage BT1 and development of site-specific integrating vectors. *J. Bacteriol.*, **185**, 5320–5323.
30. Peti,W. and Page,R. (2007) Strategies to maximize heterologous protein expression in *Escherichia coli* with minimal cost. *Protein Expr. Purif.*, **51**, 1–10.
31. Otwinowski,Z. and Minor,W. (1997) [20]Processing of X-ray diffraction data collected in oscillation mode. *Methods Enzymol.*, **276**, 307–326.
32. Xu,D., Jaroszewski,L., Li,Z. and Godzik,A. (2014) FFAS-3D: improving fold recognition by including optimized structural features and template re-ranking. *Bioinformatics*, **30**, 660–667.
33. Stein,N. (2008) CHAINSAW: a program for mutating pdb files used as templates in molecular replacement. *J. Appl. Crystallogr.*, **41**, 641–643.
34. McCoy,A.J. (2007) Solving structures of protein complexes by molecular replacement with Phaser. *Acta Crystallogr. D Biol. Crystallogr.*, **63**, 32–41.
35. Emsley,P., Lohkamp,B., Scott,W.G. and Cowtan,K. (2010) Features and development of Coot. *Acta Crystallogr. D Biol. Crystallogr.*, **66**, 486–501.
36. Adams,P.D., Afonine,P.V., Bunkoczi,G., Chen,V.B., Davis,I.W., Echols,N., Headd,J.J., Hung,L.W., Kapral,G.J., Grosse-Kunstleve,R.W. *et al.* (2010) PHENIX: a comprehensive Python-based system for macromolecular structure solution. *Acta Crystallogr. D Biol. Crystallogr.*, **66**, 213–221.
37. Chen,V.B., Arendall,W.B. 3rd, Headd,J.J., Keedy,D.A., Immormino,R.M., Kapral,G.J., Murray,L.W., Richardson,J.S. and Richardson,D.C. (2010) MolProbity: all-atom structure validation for macromolecular crystallography. *Acta Crystallogr. D Biol. Crystallogr.*, **66**, 12–21.
38. Keller,S., Vargas,C., Zhao,H., Piszczek,G., Brautigam,C.A. and Schuck,P. (2012) High-precision isothermal titration calorimetry with automated peak-shape analysis. *Anal. Chem.*, **84**, 5066–5073.
39. Houtman,J.C., Brown,P.H., Bowden,B., Yamaguchi,H., Appella,E., Samelson,L.E. and Schuck,P. (2007) Studying multisite binary and ternary protein interactions by global analysis of isothermal titration calorimetry data in SEDPHAT: application to adaptor protein complexes in cell signaling. *Protein Sci.*, **16**, 30–42.
40. Muller,F., Voordouw,G., Berkel,W.J.H., Steennis,P.J., Visser,S. and Rooijen,P.J. (1979) A study of *p*-hydroxybenzoate hydroxylase from *Pseudomonas fluorescens*. improved purification, relative molecular mass, and amino acid composition. *Eur. J. Biochem.*, **101**, 235–244.
41. Bentley,S.D., Chater,K.F., Cerdeno-Tarraga,A.M., Challis,G.L., Thomson,N.R., James,K.D., Harris,D.E., Quail,M.A., Kieser,H., Harper,D. *et al.* (2002) Complete genome sequence of the model actinomycete *Streptomyces coelicolor* A3(2). *Nature*, **417**, 141–147.
42. Altschul,S.F., Gish,W., Miller,W., Myers,E.W. and Lipman,D.J. (1990) Basic local alignment search tool. *J. Mol. Biol.*, **215**, 403–410.
43. Finn,R.D., Clements,J. and Eddy,S.R. (2011) HMMER web server: interactive sequence similarity searching. *Nucleic Acids Res.*, **39**, W29–W37.
44. Jaroszewski,L., Li,Z., Cai,X.H., Weber,C. and Godzik,A. (2011) FFAS server: novel features and applications. *Nucleic Acids Res.*, **39**, W38–W44.
45. Strohl,W.R. (1992) Compilation and analysis of DNA sequences associated with apparent streptomycete promoters. *Nucleic Acids Res.*, **20**, 961–974.
46. Larkin,M.A., Blackshields,G., Brown,N.P., Chenna,R., McGettigan,P.A., McWilliam,H., Valentin,F., Wallace,I.M., Wilm,A., Lopez,R. *et al.* (2007) Clustal W and Clustal X version 2.0. *Bioinformatics*, **23**, 2947–2948.
47. Thompson,W. (2003) Gibbs Recursive Sampler: finding transcription factor binding sites. *Nucleic Acids Res.*, **31**, 3580–3585.
48. Molina-Henares,A.J., Krell,T., Eugenia Guazzaroni,M., Segura,A. and Ramos,J.L. (2006) Members of the IclR family of bacterial transcriptional regulators function as activators and/or repressors. *FEMS Microbiol. Rev.*, **30**, 157–186.
49. Tropel,D. and van der Meer,J.R. (2004) Bacterial transcriptional regulators for degradation pathways of aromatic compounds. *Microbiol. Mol. Biol. Rev.*, **68**, 474–500.
50. Lorca,G.L., Ezersky,A., Lunin,V.V., Walker,J.R., Altamentova,S., Evdokimova,E., Vedadi,M., Bochkarev,A. and Savchenko,A. (2007) Glyoxylate and pyruvate are antagonistic effectors of the *Escherichia coli* IclR transcriptional regulator. *J. Biol. Chem.*, **282**, 16476–16491.
51. Crooks,G.E., Hon,G., Chandonia,J.M. and Brenner,S.E. (2004) WebLogo: a sequence logo generator. *Genome Res.*, **14**, 1188–1190.